数理解析研究所講究録
第1671巻 2009年 45-63

Quantum Turbulence

大阪市立大学・大学院理学研究科 坪田 誠(Makoto Tsubota)
Department of Physics、 Faculty of Science
Osaka City University

1. Introduction

About 500 years ago Leonard da Vinci observed turbulent flow of water and drew a sketch showing that turbulence was comprised of lots of vortices (Fig.1). Turbulence is still one of the important unresolved problems in nature, while it is very difficult to understand because turbulence is very complicated and nonlinear phenomena. The concept of "vortex " may be a key issue, but it is not straightforward to identify vortices in a usual classical fluid and to know the relation between turbulence and vortices.[1)]

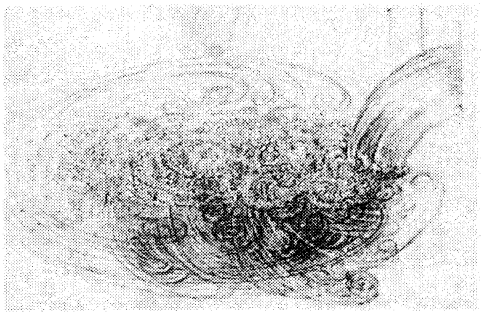

Fig.1 Sketch of turbulence by Da Vinci.

On the other hand, in the field of low temperature physics, turbulence of superfluid helium has been studied for these 50 years. Liquid helium enters the superfluid state below 2.17 K because of Bose-Einstein

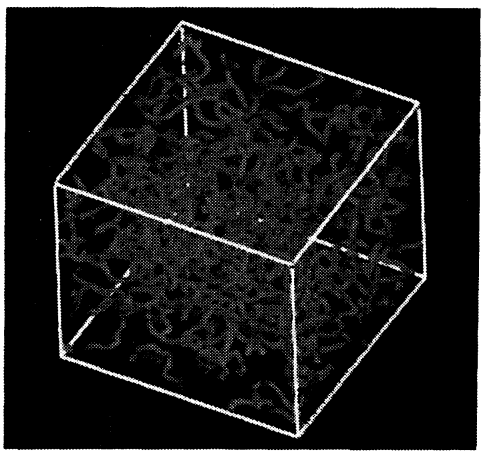

Fig.2 Quantum turbulence. The lines show the cores of quantized vortices.

condensation of helium atoms. This state is subject to severe constraints of quantum mechanics. The most important feature is that circulation of every vortex is quantized by the quantum h/m, where h is Planck's constant and m is the mass of an atom. Such a vortex is called *quantized vortex*, being a stable topological defect. Even in superfluid helium occurs turbulence, which is comprised of quantized vortices and called *quantum turbulence* (Fig.2).

Recently there have been growing interests on quantum turbulence.[2] Since quantum turbulence consists of definite elements (quantized vortices), it is expected to give a prototype of turbulence much simpler than conventional classical turbulence and to make a breakthrough for the great mystery of nature. I will discuss this fascinating topic briefly.

2. Bose-Einstein condensation, superfluidity, and quantized vortices

This section reviews briefly the backgrounds of low temperature physics necessary for understanding this article.

2.1 Bose-Einstein condensation

Quantum mechanics, which has developed since the beginning of the 20th century, has changed drastically our natural philosophy. Quantum mechanics is often thought to give the physical laws at microscopic scales, but this understanding is not necessarily correct. Quantum mechanics actually obeys the physical laws even at macroscopic scales. Such a field is quantum statistical mechanics.

The essence of quantum mechanics is the duality of particle-picture and wave-picture. Let's consider an ideal atomic gas. At relatively high temperatures, the statistics of the atoms obeys the classical Maxwell-Boltzman distribution

and each atom behaves like a particle. As the temperature is reduced, however, the thermal de Broglie wavelength is increased to become comparable to the mean distance between atoms. Then each atom becomes to behave like a wave, and the statistics changes to the quantum Fermi-Dirac or Bose-Einstein distribution depending on whether the atom is a Fermion or a Boson. If the atoms are Bosons and the system is cooled below a critical temperature T_{BEC}, they cause Bose-Einstein condensation in which these atoms occupy the same single-particle ground state [3] ; the critical temperature is given by

$$T_{BEC} = 3.3\frac{\hbar^2 n^{2/3}}{mk_B} \tag{1}$$

where the relevant quantities are the particle mass m, the number density n, the Planck constant $h = 2\pi\hbar$, and the Boltzman constant k_B.

Then matter-waves of atoms become coherent to make a macroscopic wave function (the order parameter) $\Psi(\mathbf{r}) = \sqrt{n_0(\mathbf{r})}\exp(i\theta(\mathbf{r}))$ extending over the whole volume of the system, and the assemblage of these atoms is called a Bose-Einstein condensate (BEC). Thus quantum mechanics appears at macroscopic scales through Bose-Einstein condensation.

Bose-Einstein condensation was theoretically predicted by Einstein in 1925. However, nobody knew in those days a system in which Bose-Einstein condensation occurs actually.

2.2 Liquid helium and superfludity

Independently of these studies in quantum statistical mechanics, the field of low temperature physics has developed since the beginning of 20th century. Low temperature physics is generally believed to start with the first liquefaction of ^{4}He at 4.2K by Onnes in 1908. Subsequently, Onnes observed superconductivity in mercury in 1911. Onnes noticed the

anomaly of heat capacity of liquid helium at the λ point T_λ=2.17K too. In 1938 Kapitza *et al.* observed that liquid ^{4}He becomes inviscid below the point and called this striking phenomenon *superfluidity*.

London proposed theoretically in 1938 that the λ transition is caused by Bose-Einstein condensation of ^{4}He atoms. When T_{BEC} of Eq. (1) is evaluated for the mass and density appropriate to liquid ^{4}He at saturated vapor pressure, one obtains T_{BEC} of approximately 3.13K, which is close to T_λ=2.17K.

2.3 Two-fluid model and a quantized vortex

In order to explain various hydrodynamic phenomena of superfluidity, Tisza and Landau introduced the two-fluid model. According to the two-fluid model, the system consists of an inviscid superfluid (density ρ_s) and a viscous normal fluid (density ρ_n) with two independent velocity fields $\mathbf{v}_s$ and $\mathbf{v}_n$. The mixing ratio of the two fluids depends on temperature. As the temperature is reduced below the λ point, the ratio of the superfluid component increases, and the entire fluid becomes a superfluid below approximately 1K. The Bose-condensed system exhibits the macroscopic wave function $\Psi(\mathbf{r})=\sqrt{n_0(\mathbf{r})}\exp(i\theta(\mathbf{r}))$ as an order parameter. The superfluid velocity field is given by $\mathbf{v}_s(\mathbf{r})=(\hbar/m)\nabla\theta(\mathbf{r})$ with boson mass m, representing the potential flow. Since the macroscopic wave function should be single-valued for the space coordinate $\boldsymbol{r}$, the circulation $\Gamma=\oint v_s(\mathbf{r})\cdot d\mathbf{r}$ for an arbitrary closed loop in the fluid is quantized by the quantum $\kappa=h/m$. A vortex with such quantized circulation is called a quantized vortex. Any rotational motion of a superfluid is sustained only by quantized vortices. A quantized vortex was predicted by Feynman [4] and observed experimentally in helium by Vinen.

A quantized vortex is a topological defect characteristic of a Bose--Einstein condensate and is different from a vortex in a

classical viscous fluid. First, the circulation is quantized, which is contrary to a classical vortex that can have any value of circulation. Second, a quantized vortex is a vortex of inviscid superflow. Thus, it cannot decay by the viscous diffusion of vorticity that occurs in a classical fluid. Third, the core of a quantized vortex is very thin, on the order of the coherence length, which is only a few angstroms in superfluid ^{4}He. Since the vortex core is very thin and does not decay by diffusion, it is always possible to identify the position of a quantized vortex in the fluid. These properties make a quantized vortex more stable and definite than a classical vortex.

2.4 Early studies on superfluid turbulence

Early experimental studies on superfluid turbulence focused primarily on thermal counterflow, in which the normal fluid and superfluid flow in opposite directions. The flow is driven by an injected heat current, and it was found that the superflow becomes dissipative when the relative velocity between the two fluids exceeds a critical value. Feynman proposed that this is a superfluid turbulent state consisting of a tangle of quantized vortices[4]. Vinen later confirmed Feynman's findings experimentally by showing that the dissipation comes from the mutual friction between vortices and the normal. Subsequently, several experimental studies have examined superfluid turbulence (ST) in thermal counterflow systems and have revealed a variety of physical phenomenon. Since the dynamics of quantized vortices is nonlinear and non-local, it has not been easy to understand vortex dynamics observations quantitatively. Schwarz clarified the picture of ST consisting of tangled vortices by a numerical simulation of the quantized vortex filament model in the thermal counterflow [5]. However, since the thermal counterflow has no analogy to conventional fluid dynamics, this study was

not helpful in clarifying the relationship between ST and classical turbulence (CT). Superfluid turbulence is often called quantum turbulence (QT), which emphasizes the fact that it is comprised of quantized vortices.

3. Classical turbulence and quantum turbulence

Before considering QT, we briefly review classical fluid dynamics and the statistical properties of CT [1], then compare CT and QT.

3.1 Statistical properties of classical turbulence

Classical viscous fluid dynamics is described by the Navier--Stokes equation:

$$\frac{\partial}{\partial t}\mathbf{v}(\mathbf{r},t)+\mathbf{v}(\mathbf{r},t)\cdot\nabla\mathbf{v}(\mathbf{r},t)=-\frac{1}{\rho}\nabla P(\mathbf{r},t)+\nu\nabla^2(\mathbf{r},t) \qquad (2)$$

where $\mathbf{v}(\mathbf{r},t)$ is the velocity of the fluid, $P(\mathbf{r},t)$ is the pressure, ρ is the density of the fluid, and ν is the kinematic viscosity. The flow of this fluid can be characterized by the ratio of the second term of the left-hand side of Eq.(2), hereinafter referred to as the inertial term, to the second term of the right-hand side, hereinafter called the viscous term. This ratio is the Reynolds number $R=\bar{v}D/\nu$, where $\bar{v}$ and D are the characteristic velocity of the flow and the characteristic scale, respectively. When $\bar{v}$ increases to allow the Reynolds number to exceed a critical value, the system changes from a laminar state to a turbulent state, in which the flow is highly complicated and contains many eddies.

Such turbulent flow is known to show characteristic statistical behavior [6]. We assume a steady state of fully developed turbulence of an incompressible classical fluid. The energy is injected into the fluid at a rate of ε, the scale of which is comparable to the system size in the energy-containing range. In the inertial range, this energy is transferred to smaller scales without being dissipated. In this

range, the system is locally homogeneous and isotropic, which leads to the statistics of the energy spectrum known as the Kolmogorov law:

$$E(k) = C\varepsilon^{2/3}k^{-5/3} \tag{3}$$

Here, the energy spectrum $E(k)$ is defined as $E = \int dk E(k)$, where E is the kinetic energy per unit mass and k is the wavenumber from the Fourier transformation of the velocity field. The spectrum of Eq. (3) is easily derived by assuming that $E(k)$ is locally determined by only the energy flux ε and k. The energy transferred to smaller scales in the energy-dissipative range is dissipated at the Kolmogorov wavenumber $k_K = (\varepsilon/\nu^3)^{1/4}$ through the viscosity of the fluid with dissipation rate ε, which is equal to the energy flux in the inertial range. The Kolmogorov constant C is a dimensionless parameter of order unity. The Kolmogorov spectrum is confirmed experimentally and numerically in turbulence at high Reynolds numbers. The inertial range is thought to be sustained by the self-similar Richardson cascade in which large eddies are broken up into smaller eddies through many vortex reconnections. In CT, however, the Richardson cascade is not completely understood because it is impossible to definitely identify each eddy.

3.2 Classical turbulence and quantum turbulence

Comparing QT and CT reveals definite differences. Turbulence in a classical viscous fluid appears to be comprised of vortices, as pointed out by da Vinci. However, these vortices are unstable, repeatedly appearing and disappearing. Moreover, the circulation is not conserved and is not identical for each vortex. Quantum turbulence consists of a tangle of quantized vortices that have the same conserved circulation. Looking back at the history of science, *reductionism*, which tries to understand the nature of complex things by reducing them to the interactions of their parts, has played an extremely

important role. The success of solid state physics owes much to *reductionism*. In contrast, conventional fluid physics is not reducible to elements, and thus does not enjoy the benefits of *reductionism*. However, quantum turbulence is different, being reduced to quantized vortices. Thus *reductionism* is applicable to quantum turbulence. Consequently, QT should lead to a simpler model of turbulence than CT.

3.3 Research trends of quantum hydrodynamics

Based on these considerations, research into quantum hydrodynamics has opened up new directions since the mid 1990s. One new direction has occurred in the field of low temperature physics by studying superfluid helium. It started with the attempt to understand the relationship between QT and CT [7]. Recent experimental and numerical studies support a Kolmogorov spectrum in QT. Following these studies, QT research on superfluid helium has moved to important topics such as the dissipation process at very low temperatures, QT created by vibrating structures, and visualization of QT [7]. Another new direction is the realization of Bose-Einstein condensation in trapped atomic gases in 1995, which has stimulated intense experimental and theoretical activity [3]. As proof of the existence of superfluidity, quantized vortices have been created and observed in atomic BECs, and numerous efforts have been devoted to a number of fascinating problems [7]. Atomic BECs have several advantages over superfluid helium. The most important is that modern optical techniques enable one to directly control condensates and visualize quantized vortices. A series of experiments on BECs clearly show the properties of quantum hydrodynamics.

4. Quantized vortices in a rotating BEC

This section describes the typical phenomenon of quantum hydrodynamics of atomic BECs, namely the vortex lattice

formation in a rotating BEC. What happens if we rotate a cylindrical vessel with a classical viscous fluid inside? Even if the fluid is initially at rest, it starts to rotate and eventually reaches a steady rotation with the same rotational speed as the vessel. In that case, one can say that the system contains a vortex that mimics solid-body rotation. A rotation of arbitrary angular velocity can be sustained by a single vortex. However, this does not occur in a quantum fluid. .Because of quantization of circulation, superfluids respond to rotation, not with a single vortex, but with a lattice of quantized vortices. Feynman noted that in uniform rotation with angular velocity Ω the rot of the superfluid velocity is the circulation per unit area, and since the rot is 2Ω, a lattice of quantized vortices with number density $n_0 = \mathrm{rot}\,\mathbf{v}_s/\kappa = 2\Omega/\kappa$ ("Feynman's rule") arranges itself parallel to the rotation axis ¥cite{Feynman}. Such experiments were performed for superfluid ^{4}He: Packard *et al.* visualized vortex lattices on the rotational axis by trapping electrons along the cores.

This idea has also been applied to atomic BECs. Several groups have observed vortex lattices in rotating BECs. Among them, Madison *et al.* directly observed nonlinear processes such as vortex nucleation and lattice formation in a rotating ^{87}Rb BEC [8].

By sudden application of a rotation along the trapping potential, an initially axisymmetric condensate undergoes a collective quadrupole oscillation to an elliptically deformed condensate. This oscillation continues for a few hundred milliseconds with gradually decreasing amplitude. Then the axial symmetry of the condensate is recovered and vortices enter the condensate through its surface, eventually settling into a lattice configuration.

This observation has been reproduced by a simulation of the Gross-Pitaevskii (GP) equation for the macroscopic wave

function $\Psi(\mathbf{r},t)$. The corresponding GP equation in a frame rotating with frequency $\Omega = \Omega\hat{z}$ is given by

$$(i-\gamma)\hbar\frac{\partial\Psi(\mathbf{r},t)}{\partial t} = \left[-\frac{\hbar^2}{2m}\nabla^2 + V_{ex}(\mathbf{r}) + g\left|\Psi(\mathbf{r},t)\right|^2 - \Omega L_z\right]\Psi(\mathbf{r},t). \tag{4}$$

Here V_{ex} is a trapping potential, and $L_z = -i\hbar\left(x\partial_y - y\partial_x\right)$ is the angular momentum along the rotational axis. The interparticle potential is approximated by a short-range interaction $V \approx g\delta(\mathbf{r}-\mathbf{r}')$. The term γ indicates phenomenological dissipation.

Figure 3 shows the profile of the condensate density $\left|\Psi(\mathbf{r})\right|^2$ and the phase $\theta(\mathbf{r})$ when there is a quantized vortex in a trapped BEC. The density has a hole representing the vortex core. The phase has a branch cut between 0 and 2π, and the edge of the branch cut corresponds to the vortex core around which the phase rotates by 2π as the superflow circulates. One can therefore clearly identify the vortex both in the density and the phase.

A typical two-dimensional numerical simulation of Eq. (4) for

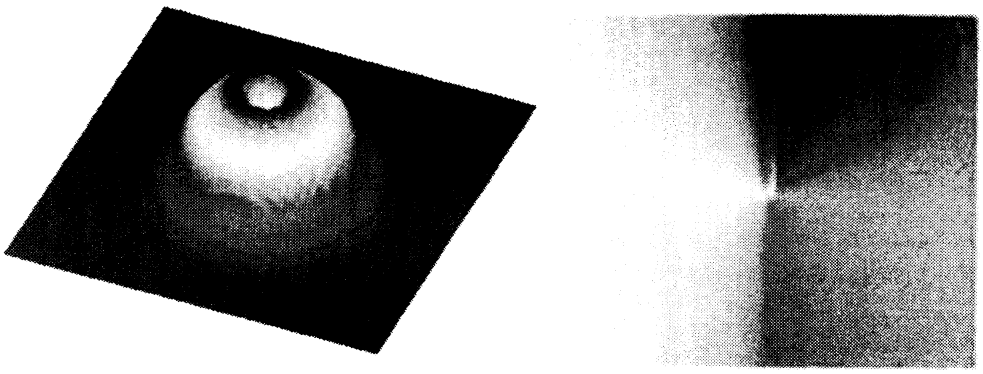

(a) (b)

Fig.3 Profile of (a) the condensate density and (b) the phase of the macroscopic wavefunction when there is a quantized vortex in a trapped BEC. The value of the phase varies continuously from 0 (red) to 2π (blue).

the vortex lattice formation is shown in Fig. 4 [9], where the condensate density and the phase are displayed together. We first prepare an equilibrium condensate trapped in a stationary potential. When we apply a rotation, the condensate becomes elliptic and performs a quadrupole oscillation [Fig. 4(a)]. Then, the boundary surface of the condensate becomes unstable and generates ripples that propagate along the surface [Fig. 4(b)]. As stated previously, it is possible to identify quantized vortices in the phase profile also. As soon as the rotation starts, many vortices appear in the low-density region outside of the condensate [Fig. 4(a)]. Since quantized vortices are excitations, their nucleation increases the energy of the system. Because of the low density in the outskirts of the condensate, however, their nucleation contributes little to the energy and angular momentum. Since these vortices outside of the condensate are not observed in the density profile, they are called "ghost vortices". Their movement toward the Thomas-Fermi surface excites ripples [Fig. 4(b)]. It is not easy for these ghost vortices to enter the condensate, because that would increase both the energy and angular momentum. Only some vortices enter the condensate cloud to become "real vortices" wearing the usual density profile of quantized vortices [Fig. 4(d)], eventually forming a vortex lattice [Fig. 4 (e) and (f)]. The number of vortices forming a lattice is given by "Feynman's rule". The numerical results agree quantitatively with these observations.

Note the essence of the dynamics. The initial state has no vortices in the absence of rotation. The final state is a vortex lattice corresponding to rotational frequency Ω. In order to go from the initial to the final state, the system makes use of as many excitations as possible, such as vortices, quadruple oscillation, and surface waves. We refer the readers to Ref. 9 for details.

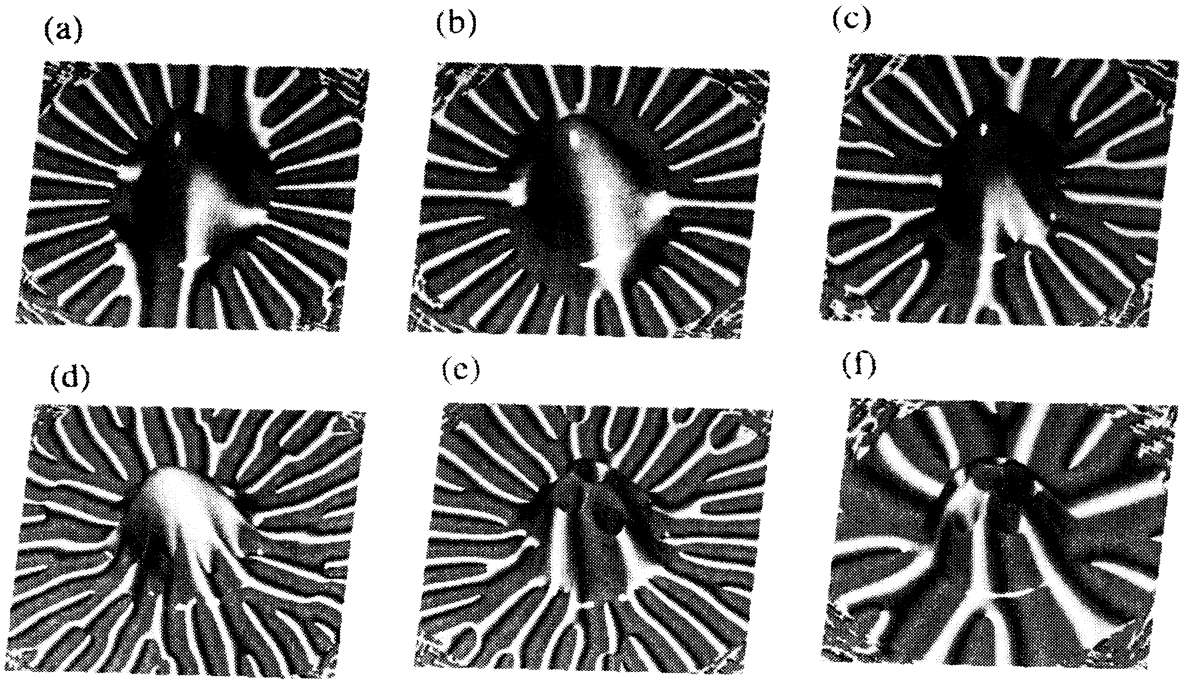

Fig.4 Dynamics of vortex lattice formation in a rotating BEC. The figure simultaneously shows both the condensate density and phase. They are bird's -eye pictures of the distribution of the condensate density, and the color shows the phase continuously from 0 (red) to 2π (blue). The graphs are at (a) t=63 ms, (b) 305 ms, (c) 350 ms, (d) 410 ms, (e) 450 ms, and (f) 850 ms after the start of the rotation.

5. Energy spectra of quantum turbulence

Most older experimental studies on QT were devoted to thermal counterflow. Since this flow has no classical analogue, these studies do not contribute greatly to the understanding of the relationship between CT and QT. Since the mid 1990s, important experimental, numerical theoretical studies on QT that did not focus on thermal counterflow have been published [7]. Here we will describe energy spectra of QT at zero temperature.

No experimental studies have addressed this issue directly, although a few numerical studies have been conducted. The first study was performed by Nore et al. using the GP model [10]. They solved the GP equation numerically starting

from Taylor--Green vortices, and followed the time development. The quantized vortices become tangled and the energy spectra of the incompressible kinetic energy seemed to obey the Kolmogorov law for a short period, although the energy spectra eventually deviated from the Kolmogorov law. The second study was performed by the vortex filament model [11], and the third study was performed by the modified GP model [12,13]. Here we will discuss briefly the third work.

The Kolmogorov spectra were confirmed for both decaying [12] and steady [13] QT by the modified GP model. The normalized GP equation is

$$i\frac{\partial}{\partial t}\Phi(\mathbf{x},t)=\left[-\nabla^2-\mu+g\left|\Phi(\mathbf{x},t)\right|^2\right]\Phi(\mathbf{x},t) \tag{5}$$

which determines the dynamics of the macroscopic wave $\Phi(\mathbf{x},t)=f(\mathbf{x},t)\exp[i\phi(\mathbf{x},t)]$. The condensate density is $\left|\Phi(\mathbf{x},t)\right|^2=f(\mathbf{x},t)^2$, and the superfluid velocity is given by $\mathbf{v}(\mathbf{x},t)=2\nabla\phi(\mathbf{x},t)$. The vorticity $\omega(\mathbf{x},t)=\mathrm{rot}\,\mathbf{v}(\mathbf{x},t)$ vanishes everywhere in a single-connected region of the fluid and thus all rotational flow is carried by quantized vortices. In the core of each vortex, $\Phi(\mathbf{x},t)$ vanishes so that the circulation around the core is quantized by 4π. The vortex core size is given by the healing length $\xi=1/f\sqrt{g}$.

Note that the hydrodynamics described by the GP model is compressible. The total number of condensate particles is $N=\int d\mathbf{x}\left|\Phi(\mathbf{x},t)\right|^2$ and the total energy is

$$E(t)=\frac{1}{N}\int dx\,\Phi^*(\mathbf{x},t)\left[-\nabla^2+\frac{g}{2}f(\mathbf{x},t)^2\right]\Phi(\mathbf{x},t), \tag{6}$$

which is represented by the sum of the interaction energy $E_{\mathrm{int}}(t)$, the quantum energy $E_q(t)$, and the kinetic energy $E_{kin}(t)$ [10]:

$$E_{\mathrm{int}}(t)=\frac{g}{2N}\int d\mathbf{x}\,f(\mathbf{x},t)^4,\quad E_q(t)=\frac{1}{N}\int d\mathbf{x}\left[\nabla f(\mathbf{x},t)\right]^2,\quad E_{kin}(t)=\frac{1}{N}\int d\mathbf{x}\left[f(\mathbf{x},t)\nabla\phi(\mathbf{x},t)\right]^2. \tag{7}$$

The kinetic energy is furthermore divided into a compressible part $E^c_{kin}(t)$ due to compressible excitations and an incompressible part $E^i_{kin}(t)$ due to vortices. If the Kolmogorov spectrum is observed, the spectrum should be that for the incompressible kinetic energy.

Nore *et al.* tried to obtain the Kolmogorov spectrum from the pure GP equation, not succeeding [10]. The failure would be attributable to the following reasons. Note that the situation they studied was decaying turbulence. Although the total energy $E(t)$ was conserved, $E^i_{kin}(t)$ decreased with increasing $E^c_{kin}(t)$. This was because many compressible excitations were created through repeated vortex reconnections and disturbed the Richardson cascade of quantized vortices even at large scales.

Kobayashi and Tsubota overcame the difficulties of Nore {¥it et al.} and obtained the Kolmogorov spectra in QT and clearly revealed the energy cascade [12,13]. They performed numerical calculation for the Fourier transformed GP equation with dissipation:

$$\left(i-\tilde{\gamma}(\mathbf{k})\right)\frac{\partial}{\partial t}\tilde{\Phi}(\mathbf{k},t)=\left[k^2-\mu(t)\right]\tilde{\Phi}(\mathbf{k},t)+\frac{g}{V^2}\sum_{\mathbf{k}_1,\mathbf{k}_2}\tilde{\Phi}(\mathbf{k}_1,t)\tilde{\Phi}^*(\mathbf{k}_2,t)\tilde{\Phi}(\mathbf{k}-\mathbf{k}_1+\mathbf{k}_2,t) \quad (8)$$

Here, $\tilde{\Phi}(\mathbf{k},t)$is the spatial Fourier component of $\Phi(\mathbf{x},t)$ and V is the system volume. The dissipation should have the form $\tilde{\gamma}(\mathbf{k})=\gamma_0\theta(k-2\pi/\xi)$with the step function θ, which dissipates only the excitations smaller than ξ. This form of dissipation can be justified by the coupled analysis of the GP equation for the macroscopic wave function and the Bogoliubov--de Gennes equations for thermal excitations.

First, Kobayashi and Tsubota confirmed the Kolmogorov spectra for decaying turbulence [12]. To obtain a turbulent state, they started the calculation from an initial configuration in which the density was uniform and the phase of the wave function had a random spatial distribution. The initial wave

function was dynamically unstable and soon developed into fully developed turbulence with many quantized vortex loops. The spectrum $E^{i}_{kin}(\mathbf{k},t)$ of the incompressible kinetic energy was then found to obey the Kolmogorov law.

A more elaborate analysis of steady QT was performed by introducing energy injection at large scales as well as energy dissipation at small scales [13]. Energy injection at large scales was effected by moving a random potential $V(\mathbf{x},t)$. Numerically, Kobayashi *et al.* placed random numbers between 0 and V_0 in space-time $(\mathbf{x},t)$ at intervals of X_0 for space and T_0 for time and connected them smoothly using a four-dimensional spline interpolation. The moving random potential exhibited a Gaussian two-point correlation:

$$\langle V(\mathbf{x},t)V(\mathbf{x}',t')\rangle = V_0^2 \exp\left[-\frac{(\mathbf{x}-\mathbf{x}')^2}{2X_0^2} - \frac{(t-t'')^2}{2T_0^2}\right] . \qquad (9)$$

This moving random potential had a characteristic spatial scale of X_0 . Small vortex loops were first nucleated by the random potential, growing to the scale of X_0 by its motion subjected to Eq (9). The vortex loops were then cast into the Richardson cascade. If steady QT is obtained by the balance between the energy injection and the dissipation, it should have an energy-containing range of $k<2\pi/X_0$, an inertial range of $2\pi/X_0<k<2\pi/\xi$, and an energy-dissipative range of $2\pi/\xi<k$.

A typical simulation of steady turbulence was performed for $V_0=50$, $X_0=4\$$, and $T_0=6.4\times10^{-2}$. The dynamics started from the uniform wave function. Figure 5 shows the time development of each energy component. The moving random potential nucleates sound waves as well as vortices, but both figures show that the incompressible kinetic energy $E^{i}_{kin}(t)$ due to vortices is dominant in the total kinetic energy $E_{kin}(t)$. The four energies are almost constant for $t>25$, and steady QT was obtained.

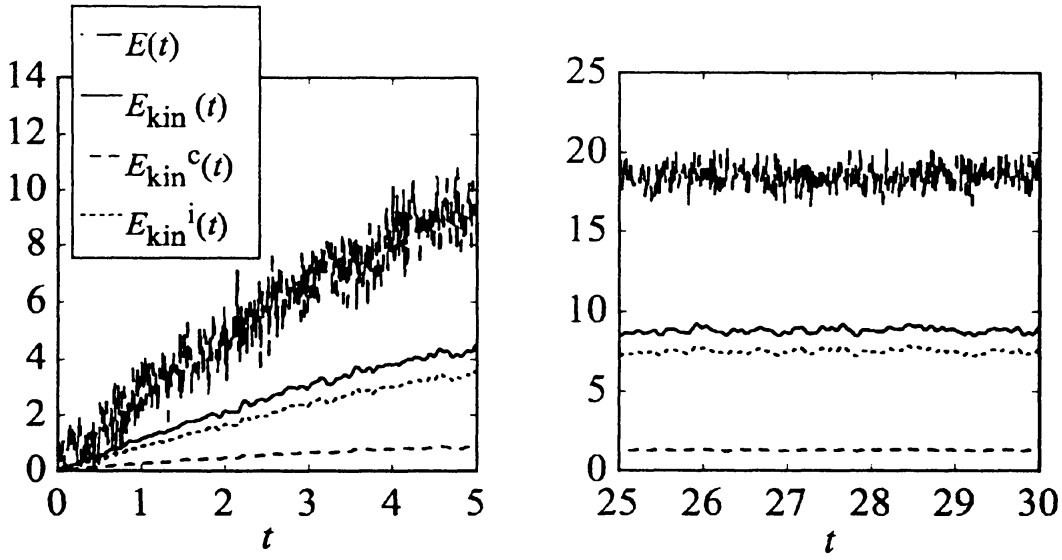

(a) (b)

Fig.5 Results of numerical simulation of the GP equation with energy injection at large scales and energy dissipation at small scales. Time development of the total energy $E(t)$, the kinetic energy $E_{kin}(t)$, the compressible kinetic energy $E^c_{kin}(t)$, and the incompressible kinetic energy $E^i_{kin}(t)$ at (a) the initial stage and (b) a later stage. The system is found to be statistically steady at the later stage.

Such a steady QT enables us to investigate the energy cascade. Here, we expect an energy flow in wavenumber space similar to that in Fig.6. The upper half of the diagram shows the kinetic energy E^i_{kin} of quantized vortices, and the lower half shows the kinetic energy E^c_{kin} of compressible excitations. In the energy-containing range $k<2\pi/X_0$, the system receives incompressible kinetic energy from the moving random potential. During the Richardson cascade process of quantized vortices, the energy flows from small to large k in the inertial range $2\pi/X_0<k<2\pi/\xi$. In the energy-dissipative range $2\pi/\xi<k$, the incompressible kinetic energy transforms to compressible kinetic energy through reconnections of vortices or the disappearance of small vortex loops. The moving random potential also creates long-wavelength compressible sound waves, which are another source of compressible kinetic

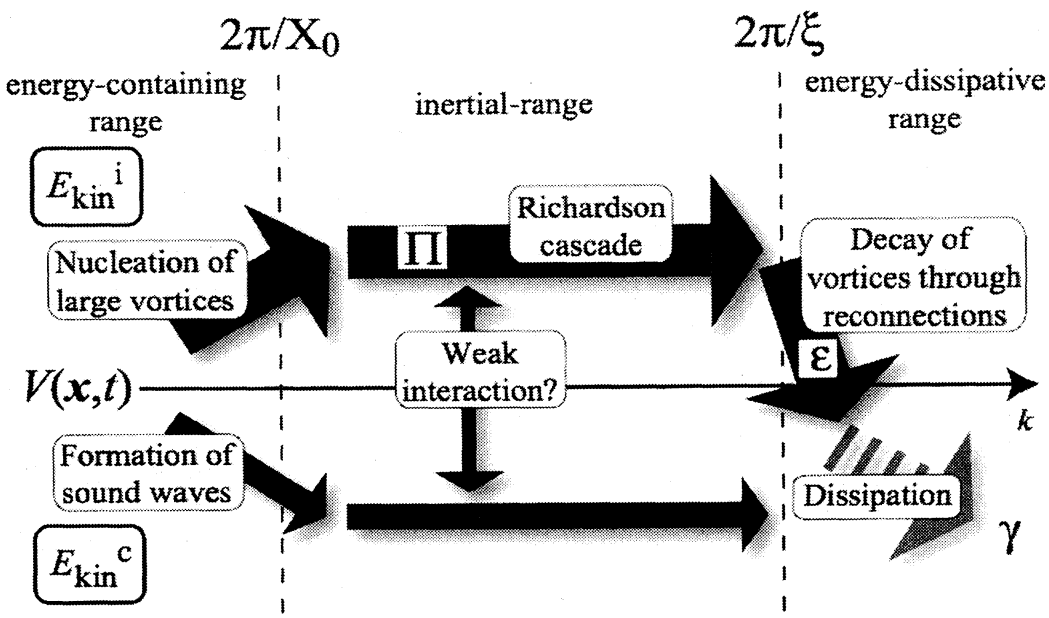

Fig. 6 Schematic diagram of the flow of the incompressible kinetic energy E^i_{kin} (upper half of diagram) and compressible kinetic energy E^c_{kin} (lower half) in wavenumber space in the steady turbulence by the GP equation¥cite. The energy is injected in the energy-containing range through the moving random potential, leading to nucleation of vortices in E^i_{kin} and formation of sound waves in E^c_{kin}. In E^i_{kin} the energy is trasferred in the inertial-range through the Richardson cascade of quantized vortices with the energy flux Π, then dissipated with the rate ε in the energy-dissipative range by the dissipative term of γ.

energy and also produce an interaction with vortices. However, the effect of sound waves is weak because E^i_{kin} is much larger than E^c_{kin}, as shown in Fig. 5.

This cascade can be confirmed quantitatively by checking whether the energy dissipation rate ε of E^i_{kin} is comparable to the flux of energy Π through the Richardson cascade in the inertial range. Although the details are described in Ref. 13, Π is found to be approximately independent of k and comparable to ε. As shown in Fig. 7, the energy spectrum is quantitatively consistent with the Kolmogorov law in the inertial range $2\pi/X_0 < k < 2\pi/\xi$. It is interesting to focus on Richardson cascade. Richardson

cascade is only conceptual in CT, while it is genuine in QT in which vortices are identified definitely. Actually we observe lots of events of the splitting of a vortex into smaller vortices in the turbulence state. The situation is more difficult to understand in CT. This is one of the reasons why we believe that QT is simper than CT.

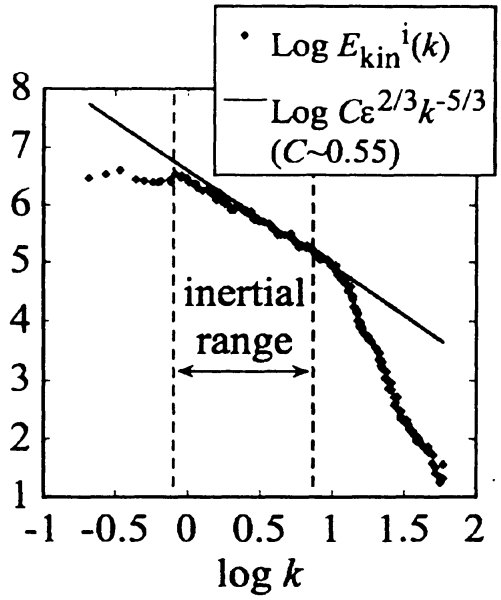

Fig.7 Energy spectrum $E_{kin}^{i}(k)$ for the steady state QT. The points are from an ensemble average of 50 randomly selected states at t>25. The solid line is the Kolmogorov law. The inertial range corresponds to $2\pi/X_0 < k < 2\pi/\xi$, in which the spectrum obeys the Kolmogorov law. The Kolmogorov constant $C \approx 0.55$ is lower than the usual value $C \approx 1.4$, the reason of which is not known.

6. Conclusions

In this article, we have reviewed recent research on quantum hydrodynamics and turbulence in superfluid helium and atomic BECs. Quantum turbulence has been long studied in superfluid helium, while it is realized experimentally in atomic BECs too very lately. Research on QT is currently one of the most important branches in low-temperature physics, attracting the attention of many scientists. QT is comprised of quantized vortices as definite elements, which differs greatly from conventional turbulence. Thus, investigation of QT may lead to a breakthrough in understanding one of the great mysteries of nature since the era of da Vinci. There are many related topics not addressed in this article, regarding which we refer the readers to other review articles [2,7].

References

1) U. Frisch: TURBULENCE (Cambridge University Press、1995).

2) M. Tsubota: J. Phys. Soc. Jpn. 77 (2008) 111006.

3) C. J. Pethick and H. Smith: Bose-Einstein Condensation in Dilute Gases (Cambridge University Press, 2nd ed., 2008).

4)R. P. Feynman: Progress in Low Temperature Physics、ed. C. J. Gorter (North-Holland、 1955) Vol. I、 p.17.

5) K. W. Schwarz: Phys. Rev. B31(1985) 5782, Phys. Rev. B 38(1988) 2398.

6)A. N. Kolmogorov: Dokl. Akad. Nauk SSSR **30** (1941) 299 [reprinted in Proc. R. Soc. A 434 (1991) 9]: A. N. Kolmogorov: Dokl. Akad. Nauk SSSR **32** (1941) 16 [reprinted in Proc. R. Soc. A 434 (1991) 15].

7)Progress in Low Temperature Physics、 ed. W. P. Halperin and M. Tsubota (Elsevier、 2008) Vol. 16.

8)K. W. Madison *et al.*: Phys. Rev. Lett. **86** (2001) 4443.

9)K. Kasamatsu, M. Tsubota and M. Ueda: Phys. Rev. A **67** (2003) 033610/

10)C. Nore *et al.*: Phys. Fluids **9** (1997) 2544.

11)T. Araki *et al.*: Phys. Rev. Lett. **89** (2002) 145301.

12)M. Kobayashi and M. Tsubota: Phys. Rev. Lett. **94** (2005) 065302.

13)M. Kobayashi and M. Tsubota: J. Phys. Soc. Jpn. **74** (2005) 3248.